GANIT *J. Bangladesh Math. Soc.* (ISSN 1606-3694) 30 (2010) 76-88

MHD HEAT AND MASS TRANSFER FREE CONVECTION FLOW ALONG A STRETCHING SHEET WITH SUCTION WHEN BUOYANCY OPPOSES THE FLOW

M. Mohebujjaman[a, b] and **M.A. Samad**[1]

[a] *Department of Mathematics,*
Bangladesh University of Engineering & Technology, Dhaka-1000
[1] *Department of Mathematics, Dhaka University, Dhaka-1000, Bangladesh*
[b] Corresponding author, Email: mjaman_du@yahoo.com

Received 23.03.09 Accepted 05.03.11

ABSTRACT

An analysis is carried out to study the flow, heat and mass transfer free convection characteristics in an electrically conducting fluid near an isothermal linearly stretching permeable vertical sheet when buoyancy force opposes the flow. The equations governing the flow, temperature and concentration field are reduced to a system of coupled non-linear ordinary differential equations. These non-linear differential equations are integrated numerically by using Nachtsheim-Swigert [1] shooting iteration technique along with sixth order Runge-Kutta integration scheme. Finally the numerical results are presented through graphs and tables.

1. Introduction

The heat, mass and momentum transport in laminar boundary layer flow over a moving continuous and linearly stretching surface has considerable practical applications in engineering, electrochemistry, D. T. Chin [2], R. S. R. Gorla [3] and polymer processing, R.M. Griffith [4], L.E. Erickson et al. [5]. For example, hot rolling, wire drawing, spinning of filaments, metal and polymer extrusion, crystal growing, continuous casting, glass fiber and paper production, drawing of plastic films etc., Altan et al. [6], Fisher [7] and Tadmor et al. [8]. It is usually assumed that the surface is inextensible, but the situations arise in the polymer industry in which it is necessary to deal with a stretching plastic sheet, as noted by Crane [9]. However, of late, hydromagnetic flow, heat and mass transfer problems have become more important industrially. To be more specific, it may be pointed out that many metallurgical processes involve the cooling of continuous strips or filaments by drawing them through a quiescent fluid and that in the process of drawing, these strips are sometimes stretched. By drawing such strips in an electrically conducting fluid subjected to a magnetic field, the rate of cooling can be controlled and a final product of desired characteristics can be achieved. Another interesting application of hydromagnetics to metallurgy lies in the purification of molten metals from nonmetallic inclusions by the application of a magnetic field. Following the pioneering work of Sakiadis [10], a rapidly increasing number of papers investigating different aspects of this problem have been published. There are fluids, which react chemically with some other

ingredients present in them. Effects of mass transfer on flow past an impulsively started infinite vertical plate with constant heat flux and chemical reaction was studied by Das et al. [11]. Anderson et al. [12] have studied the diffusion of a chemically reactive species from a linearly stretching sheet. Anjalidevi and Kandasamy [13] investigated the effects of a chemical reaction heat and mass transfer on laminar flow along a semi-infinite horizontal plate. Anjalidevi and Kandasamy [14] have analyzed the effects of a chemical reaction heat and mass transfer on MHD flow past a semi-infinite plate. McLeod and Rajagopal [15] have investigated the uniqueness of the flow of a Navier Stokes fluid due to a linear stretching boundary. Raptis et al. [16] have studied the viscous flow over a non-linearly stretching sheet in the presence of a chemical reaction and magnetic field. Suction or injection of a stretched surface was studied by Erickson et al. [5] and Fox et al. [17] for uniform surface velocity and temperature and investigated its effects on the heat and mass transfer in the boundary layer. Chen and Char [18] have studied the suction and injection on a linearly moving plate subject to uniform wall temperature and heat flux and the more general case using a power law velocity and temperature distribution at the surface was studied by Ali [19]. Magyari et al. [20] have reported analytical and computational solutions when the surface moves with rapidly decreasing velocities using the self-similar method.

In all papers mentioned above the effects of buoyancy force was relaxed. The study of heat generation or absorption in moving fluids is important in problems dealing with chemical reactions and these concerned with dissociating fluids. Possible heat generation effects may alter the temperature distribution; consequently, the particle deposition rate in nuclear reactors, electronic chips and semi conductor wafers. Vajravelu and A. Hadjinicolaou [21] studied the heat transfer characteristics in the laminar boundary layer of a viscous fluid over a stretching sheet with viscous dissipation or frictional heating and internal heat generation. The aim of this paper is to make a numerical calculation, on convective heat and mass transfer when buoyancy force opposes the flow which has been of interest to the engineering community and to the investigators dealing with the problems in geophysics, astrophysics, electrochemistry and polymer processing. From the technical point of view free convection flow past an infinite or semi-infinite vertical plate is always important for many practical applications. Usually in such types of flows, the thermal diffusion effect is neglected. In the present paper, we have investigated the effect of various dimensionless parameters on flow, heat and mass transfer characteristics of an electrically conducting viscous incompressible fluid flowing over a linearly stretching vertical sheet in the presence of a uniform magnetic field when the buoyancy force opposes the flow.

2. Mathematical Analysis

A steady-state two-dimensional heat and mass transfer flow of an electrically conducting viscous incompressible fluid along an isothermal linearly stretching vertical sheet with heat generation/absorption is considered. The stretching sheet coincides with the plane $y = 0,$ where the flow is confined to $y > 0.$ A uniform magnetic field of strength B_0 is

imposed along the y-axis. Two equal and opposite forces are introduced along the x-axis so that the sheet is stretched keeping the origin fixed as shown in Fig. 1.

The boundary-layer equations relevant to the problem considering the buoyancy force [22] are:

$$\frac{\partial u}{\partial x}+\frac{\partial v}{\partial y}=0 \tag{1}$$

$$u\frac{\partial u}{\partial x}+v\frac{\partial u}{\partial y}=\upsilon\frac{\partial^2 u}{\partial y^2}+s\,g\,\beta\,(T-T_\infty)-\frac{\sigma B_0^{\,2}u}{\rho} \tag{2}$$

$$u\frac{\partial T}{\partial x}+v\frac{\partial T}{\partial y}=\frac{\kappa}{\rho c_p}\frac{\partial^2 T}{\partial y^2}+\frac{Q_0}{\rho c_p}(T-T_\infty) \tag{3}$$

$$u\frac{\partial C}{\partial x}+v\frac{\partial C}{\partial y}=D_m\frac{\partial^2 C}{\partial y^2} \tag{4}$$

The boundary conditions for the model are

$$\left.\begin{aligned} &u=D\,x,\quad v=v_w,\quad T=T_w,\quad C=C_w \quad \text{at } y=0\\ &u=0,\quad T=T_\infty,\quad C=C_\infty \qquad\quad \text{as } y\to\infty \end{aligned}\right\} \tag{5}$$

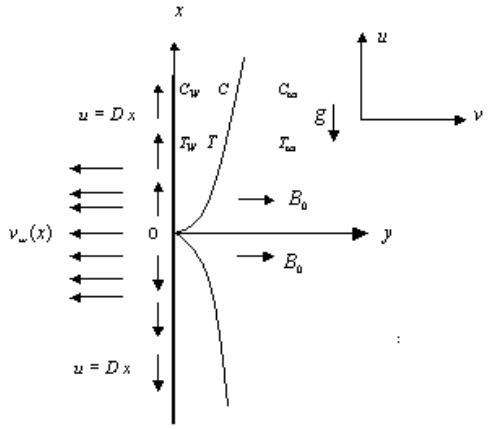

Fig. 1: Flow configuration and Coordinate system.

where u and v are the velocity components in the x and y directions respectively, υ is the kinematic viscosity, g is the acceleration due to gravity, β is the volumetric coefficient of thermal expansion, T and T_∞ are the fluid temperature within the boundary layer and in the free-stream respectively, while C is the concentration of the fluid within the boundary layer, σ is the electric conductivity, B_0 is the uniform magnetic field strength (magnetic induction), ρ is the density of the fluid, κ is the thermal conductivity of the fluid, C_p is the specific heat at constant pressure, Q_0 is the volumetric rate of heat generation/absorption and D_m is the chemical molecular diffusivity, s is a dummy

parameter stands for -1, 0, or +1. $D(>0)$ is stretching constant, v_w is a velocity component at the wall having positive value to indicate suction, T_w is the uniform wall temperature and C_w, C_∞ is the concentration of the fluid at the sheet and far from the sheet respectively. The effect of the second term on the right hand side of equation (2) is due to

buoyancy force. When $s = 0$, the buoyancy forces are neglected and the governing equations (1)-(4) reduce to those of forced convection limit. If $s = -1$, the buoyancy force is dominant and the governing equations (1)-(4) reduce to those of natural convection limit. In this case the $x-$axis points vertically downward in the direction of stretching surface but the stretching induced flow and the thermal buoyant flow oppose each other. On the other hand, when $s = +1$, the x-axis points upwards in the direction of stretching surface such that the stretching induced flow and the thermal buoyant flow assist each other. In the present investigation, we considered case when $s = -1$.

In order to obtain a solution of equations (1)-(4), we introduce the following similarity variables

$$\eta = y\sqrt{\frac{D}{\upsilon}}, \qquad \psi = \sqrt{D\upsilon}\, x f(\eta), \qquad \theta(\eta) = \frac{T - T_\infty}{T_w - T_\infty}, \qquad \phi(\eta) = \frac{C - C_\infty}{C_w - C_\infty} \tag{6}$$

where $$u = D x f'(\eta), \quad v = -\sqrt{D\upsilon}\, f(\eta) \tag{7}$$

where f', θ and ϕ are the dimensionless velocity, temperature and concentration respectively, and η is the similarity variable. By taking into account the above similarity variables, equations (1)-(4) become

$$f''' + f f'' - (f')^2 - M f' - \lambda\theta = 0 \tag{8}$$

$$\theta'' + Pr\, f\, \theta' + Pr\, Q\, \theta = 0 \tag{9}$$

$$\phi'' + S_c\, f\, \phi' = 0 \tag{10}$$

The last term in equation (8) is due to the buoyancy force and $\lambda = \dfrac{g\,\beta(T_w - T_\infty)}{D^2 x}$ which serves as the buoyancy parameter. The transformed boundary conditions are:

$$\left.\begin{array}{llll} f' = 1, & f = f_w, & \theta = 1, \phi = 1 & \text{at} \quad \eta = 0 \\ f' = 0, & \theta = 0, & \phi = 0 & \text{as} \quad \eta \to \infty \end{array}\right\} \tag{11}$$

where $f_w = -\dfrac{v_w}{\sqrt{D\upsilon}}$ is the suction parameter, $M = \dfrac{\sigma B_0^2}{\rho D}$ is the magnetic field parameter, $\Pr = \dfrac{\mu c_p}{\kappa}$ is the Prandtl number, $Q = \dfrac{Q_0}{\rho c_p D}$ is the heat source/sink

parameter, $S_c = \frac{\upsilon}{D_m}$ is the Schmidt number.

3. Numerical Computation

The numerical solutions of the non-linear system (8)-(10) under the boundary conditions (11) have been performed by applying a shooting method namely Nachtsheim-Swigert [1] iteration technique (guessing the missing boundary conditions) along with sixth order Runge-Kutta iteration scheme. The boundary conditions, equation (11), associated with the non-linear ordinary differential equations (8)-(10) are the two-point asymptotic class, that is, values of the dependent variable are specified at two different values of the independent variable. Specification of an asymptotic boundary condition implies that the first derivative (and higher derivatives of the boundary layer equation, if exists) of the dependent variable approaches zero as the outer specified value of the independent variable is approached. For the method of numerically integrating a two-point asymptotic boundary-value problem of the boundary-layer type, the initial-value method is similar to an initial value problem. Thus, it is necessary to estimate as many boundary conditions at the surface as were (previously) given at infinity. The governing differential equations are then integrated with these assumed surface boundary conditions. If the required outer boundary condition is satisfied, a solution has been achieved. However, this is not generally the case. Hence, a method must be devised to estimate logically the new surface boundary conditions for the next trial integration. Asymptotic boundary value problems such as those governing the boundary-layer equations are further complicated by the fact that the outer boundary condition is specified at infinity. In the trial integration, infinity is numerically approximated by some large value of the independent variable. There is no a priori general method of estimating these values. Selecting too small a maximum value for the independent variable may not allow the solution to asymptotically converge to the required accuracy. Selecting a large value may result in divergence of the trial integration or in slow convergence of surface boundary conditions. Selecting too large a value of the independent variable is expensive in terms of computer time. Nachtsheim-Swigert [1] developed an iteration method to overcome these difficulties. In equation (11) there are two asymptotic boundary conditions and, hence, three unknown surface conditions such as $f''(0)$, $\theta'(0)$ and $\phi'(0)$. Within the context of the initial-value method and the Nachtsheim-Swigert [1] iteration technique, the outer boundary conditions may be functionally represented as

$$Y_j(\eta_{max}) = Y_j(f''(0), \phi'(0), \theta'(0)) = \delta_j, j = 1 \cdots 6 \tag{12}$$

Where $Y_1 = f', Y_2 = \theta, Y_3 = \phi, Y_4 = f''$, $Y_5 = \theta'$ and $Y_6 = \phi'$. The last three of these represent asymptotic convergence criteria. Choosing $f''(0) = g_1$, $\theta'(0) = g_2$, $\phi'(0) = g_3$ and expanding in a first-order Taylor's series after using equation (12), we obtain

$$Y_j(\eta_{max}) = Y_{j,C}(\eta_{max}) + \sum_{i=1}^{3} \frac{\partial Y_j}{\partial g_i} \Delta g_1 = \delta_j, \qquad j = 1 \cdots 6 \tag{13}$$

where the subscript $'C'$ indicates the value of the function at η_{max} determined from the trial integration. Solution of these equations in a least-squares sense required determining the minimum value of

$$\text{Error} = \sum_{j=1}^{3} \delta_j^2 \tag{14}$$

Now differentiating (14) with respect to $g_i \quad i = 1,3$ we obtain

$$\sum_{j=1}^{6} \delta_j \frac{\partial \delta_j}{\partial g_i} = 0 \tag{15}$$

Substituting equation (13) into (15) after some algebra, we obtain

$$\sum_{k=1}^{3} a_{ik} \Delta g_i = b_i, \tag{16}$$

$$\text{where } a_{ik} = \sum_{j=1}^{6} \frac{\partial Y_j}{\partial g_i} \frac{\partial Y_j}{\partial g_k}, \quad b_i = -\sum_{j=1}^{6} Y_{j,C} \frac{\partial Y_j}{\partial g_i}, \tag{17}$$

$$i,k = 1,3$$

Now solving the system (16) using Cramer's rule, we obtain the missing (unspecified) values of g_i as

$$g_i \cong g_i + \Delta g_i. \tag{18}$$

Thus, adopting the numerical technique aforementioned along with the sixth order Runge-Kutta-Butcher initial value solver, the solutions of the equations (8)-(10) with boundary conditions (11) are obtained as a function of the coordinate η for various values of the parameters. We have chosen a step size $\Delta\eta = 0.001$ to satisfy the convergence criterion of 10^{-6} in all cases. The value of η_∞ was found to each iteration loop by $\eta_\infty = \eta_\infty + \Delta\eta$. The maximum value of η_∞ to each group of parameters f_w, M, Pr, λ, Sc, and Q determined when the value of the unknown boundary conditions at $\eta = 0$ not change to successful loop with error less than 10^{-6}.

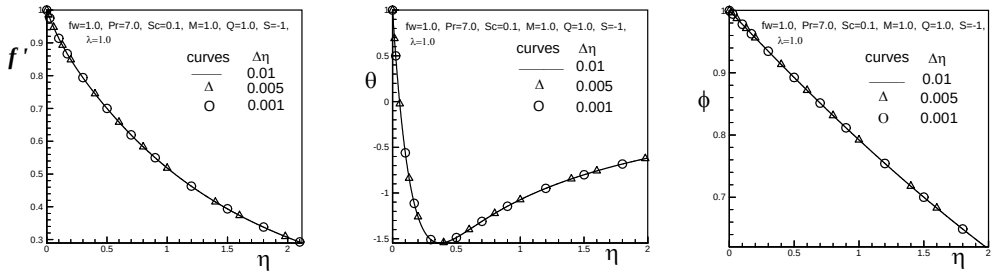

Fig. 2: (a) Velocity, (b) temperature and (c) concentration profiles for different step size $\Delta\eta$

In order to verify the effects of the step size $\Delta\eta$, we ran the code for our model with three different step sizes as $\Delta\eta = 0.01$, $\Delta\eta = 0.005$, $\Delta\eta = 0.001$ and in each case we found excellent agreement among them. The above figures show the velocity, temperature and concentration profiles for different step sizes.

4. Result and Discussion

For the purpose of discussing the result, the numerical calculations are presented in the form of non-dimensional velocity, temperature and concentration profiles. Numerical computations have been carried out for different values of the Prandtl number (Pr), Magnetic field parameter (M), Schmidt number (Sc), buoyancy parameter λ, heat source/sink parameter (Q) and Suction parameter (f_w). These are chosen arbitrarily where $\Pr = 0.71$ corresponds physically to air at 20°C, $\Pr = 1.0$ corresponds to electrolyte solution such as salt water and $\Pr = 7.0$ corresponds to water and $Sc = 0.22, 0.6$ and 1.0 corresponds to hydrogen ($Sc = 0.22$), water vapor ($Sc = 0.6$) and methanol ($Sc = 1.0$) respectively at approximate 25°C and 1 atmosphere.

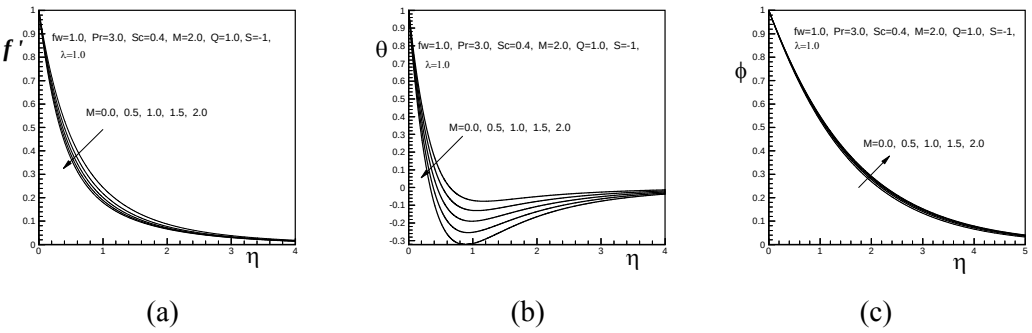

Fig. 3: (a) velocity, (b) temperature and (c) concentration profiles for different values of M

Fig. 3 displays the effects of the magnetic field parameter M on dimensionless velocity, temperature and concentration profiles. We see that velocity and temperature decrease

uniformly while concentration increases slightly with the increase of the magnetic field parameter M . The velocity gradients at the surface are negative, which signify that the stretching sheet velocity is higher than the adjacent fluid velocity. As M increases the velocity gradient at the surface decreases and this tends to reduce the shear stress at the surface, as we will see in Table1. The temperature gradient at the surface is decreasing from negative value as we increase M. Negative values of the temperature gradient signify that heat is transferred from the sheet to the ambient medium. Therefore, as we increase magnetic field parameter M , the heat transfer rate from the sheet to the environment increases, and hence it is termed as cooling processes of the sheet. Mass transfer coefficient decreases as we increase M.

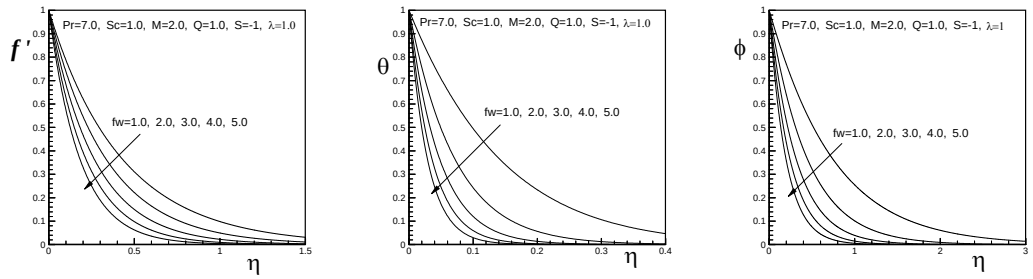

(a) (b) (c)

Fig.4: (a) velocity, (b) temperature and (c) concentration profiles for different values of f_w

Fig. 4 shows the variations of f', θ *and* ϕ for different values of suction parameter f_w. We observe that velocity, temperature and concentration decrease uniformly with the increase of suction. The figures indicate that increasing f_w reduce the hydrodynamic, thermal and concentration boundary layers thickness that in turn reduce the shear stress and increase the heat and mass transfer coefficient at the surface respectively. It is also clear from the Table1 that skin friction coefficient decreases but the heat and mass transfer coefficient increase as f_w increases. In other words, we can state that as long as suction increases the velocity of the stretching sheet increases compare to the ambient fluid velocity and the heat and mass transfer rate from the sheet to the environment increases.

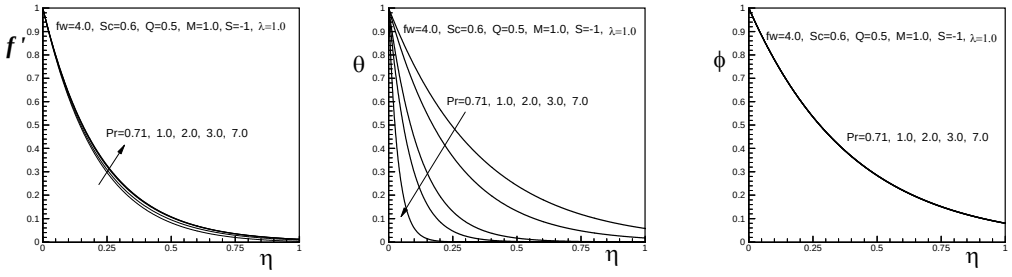

(a) (b) (c)

Fig.5: (a) velocity, (b) temperature and (c) concentration profiles for different values of Pr

The effects of Prandtl number on the velocity, temperature and concentration profiles are shown in **Fig. 5**. We observe that f' increases slightly but θ decreases rapidly with the increase of the Prandtl number, on the other hand ϕ remains same for all values of Pr. It is clear from Table2 that, the velocity gradient at the surface increases from negative value, this tend to increase the shear stress at the surface. Since the velocity gradient is negative, so the stretching velocity is higher than the adjacent fluid velocity. Fig.5 (b) indicates that increasing Pr reduces the thermal boundary layer that in turn increases the heat transfer coefficient at the surface. At $Pr = 0.71$ the temperature gradient is negative and according to equation (13) the quantity Nu_x is positive. Physically this is because the heat flows to the environment from the stretching sheet. Furthermore Nu_x increases as Pr increases. Fig.5 (c) shows the concentration profiles for the same parameters used in Fig.5 (a) and Fig.5 (b). It is clear that the concentration gradient at the surface is unchanged by changing Pr, resulting in a constant mass transfer rate. Since the concentration gradient at the surface is negative, which corresponds to the positive value of the mass transfer rate Sh, indicates that mass is transferred to the ambient medium from the sheet.

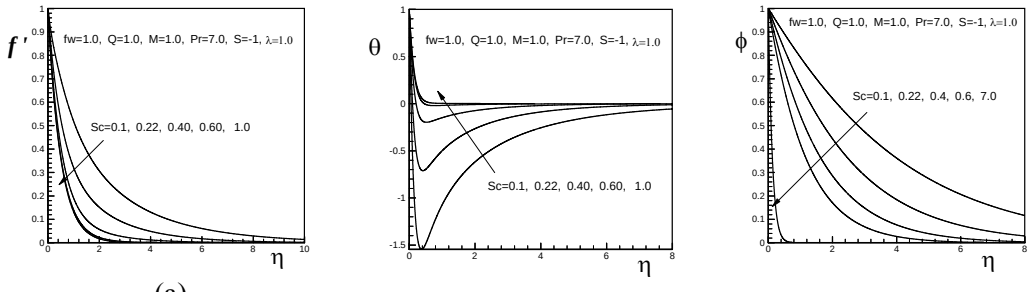

(a) (b) (c)

Fig.6: (a) velocity, (b) temperature and (c) concentration profiles for different values of Sc

Samples of the resulting velocity, temperature and concentration profiles for various values of Sc are presented in **Fig. 6.** These figures indicate that increasing Sc the velocity

and concentration gradients at the surface decrease, that in turn reduce the shear stress and increase the mass transfer coefficient at the surface respectively, also reduce the hydrodynamic and concentration boundary layers. It can be seen in Fig.6 (b) that as Sc increases, temperature gradient increases from negative value, which indicates that, the heat transfer coefficient at the decreases. From Fig.6 (a) we see that velocity gradient at the surface decreases rapidly with the small increase of Sc up to a value about 0.6, which is physically for water vapor, but when Sc gets large exceeding 0.6, the velocity gradient at the surface is unchanged by increasing Sc , resulting in a constant shear stress.

Fig. 7 displays the dimensionless velocity, temperature and concentration profiles for several values of heat source/sink parameter Q. It shows that velocity increases but the temperature and concentration decrease with the increase of heat source/sink parameter Q.

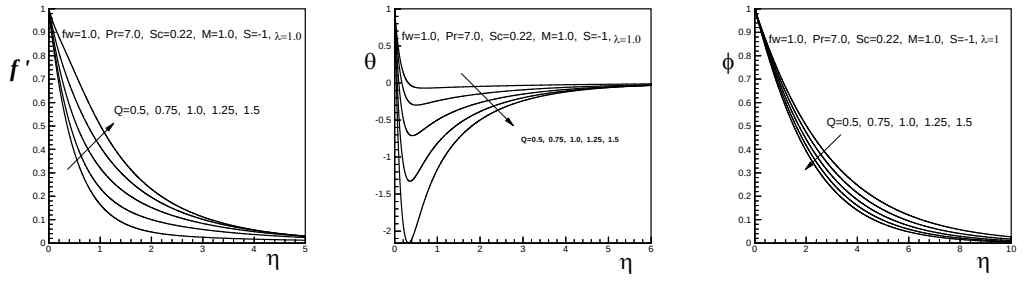

(a) (b) (c)

Fig.7: (a) velocity, (b) temperature and (c) concentration profiles for different values of Q

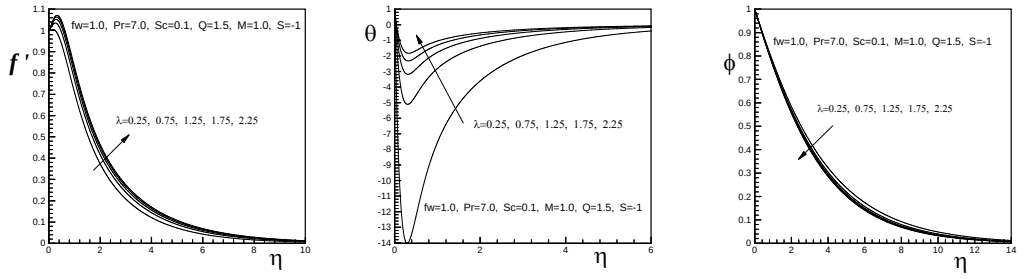

(a) (b) (c)

Fig.8: (a) velocity, (b) temperature and (c) concentration profiles for different values of λ

The effects of buoyancy parameter λ on f', θ and ϕ are shown in Fig .8. We observe that θ increases rapidly but f' increases slowly with the increase of the buoyancy

parameter λ. On the other hand concentration decreases slowly with the increase of λ. It is clear from Fig. 8 (a) that the velocity gradient at the surface increases from negative to a positive value as λ increases. The critical value of $\lambda = \lambda_{(crt.)} \approx 0.32084$ is for zero velocity gradient ($C_f \approx 0.0000026$).

The parameters of engineering interest for the present problem are the skin friction coefficient (C_f), local Nusselt number(Nu_x) and the local Sherwood number (Sh), which indicate physically wall shear stress, local wall heat transfer rate and wall mass transfer rate respectively. The skin-friction coefficient is given by

$$c_f = \frac{2}{\sqrt{\mathrm{Re}}} f''(0) \tag{19}$$

The local heat transfer coefficient is defined as $Nu_x = -\sqrt{\mathrm{Re}}\,\theta'(0)$ (20)

The local Sherwood number (Sh) is obtained as $Sh = -\sqrt{\mathrm{Re}}\,\phi'(0)$ (21)

Thus from equations (19) - (21) the values proportional to the skin-friction coefficient, Nusselt number and Sherwood number are $f''(0)$, $-\theta'(0)$ and $-\phi'(0)$ respectively. The numerical values proportional to C_f, Nu_x and Sh, calculated from equations (12) - (14) are shown in Table1- Table 3.

Table 1: C_f, Nu_x and Sh for different values of M, f_w.

M	C_f	Nu_x	Sh	f_w	C_f	Nu_x	Sh
0.0	-1.7334133	3.2711356	0.5948853	1.0	-2.4171829	6.7820175	1.2728272
0.5	-1.9015146	3.5660539	0.5851370	2.0	-3.0650759	13.9130332	2.1910365
1.0	-2.0454931	3.8854003	0.5782359	3.0	-3.8365619	20.9471928	3.1440147
1.5	-2.1746728	4.2180024	0.5728744	4.0	-4.6803058	27.9613010	4.1145135
2.0	-2.2936922	4.5569352	0.5684674	5.0	-5.5692076	34.9690164	5.0945688

Table 2: C_f, Nu_x and Sh for different values of Pr, Sc.

Pr	C_f	Nu_x	Sh	Sc	C_f	Nu_x	Sh
.71	-4.7581015	2.8079985	2.4822969	0.10	-1.0215458	21.7654573	0.2214358
1.0	-4.6728301	3.9911330	2.4843733	0.22	-1.5853362	13.9051040	0.3705426
2.0	-4.5652171	8.0352359	2.4863932	0.40	-1.9544137	8.9472333	0.5765900
3.0	-4.5280561	12.057006	2.4868545	0.60	-2.0969148	7.0693779	0.8123174
7.0	-4.4841264	28.090279	2.4872035	1.00	-2.1176988	6.7970521	1.2943868

Table 3: C_f, Nu_x and Sh for different values of Q, λ.

Q	C_f	Nu_x	Sh	λ	C_f	Nu_x	Sh
0.50	-2.0410162	7.9434734	0.3269039	0.25	-0.0357216	144.1784706	0.2425526
0.75	-1.8572139	9.9898337	0.3484086	0.75	0.1095936	57.3181339	0.2515904
1.00	-1.5853362	13.9051040	0.3705426	1.25	0.1546736	38.5044005	0.2559462
1.25	-1.2385732	19.9671688	0.3916959	1.75	0.1665122	30.0975110	0.2587630
1.50	-0.8245295	28.4402787	0.4116685	2.25	0.1601469	25.2796245	0.2607496

Conclusion

Heat and mass transfer characteristics of a linearly stretching vertically moving permeable stretching sheet are studied when $s = -1$ which means that the x-axis points vertically downwards in the direction of stretching the hot surface such that the stretching induced flow and the thermal buoyant flow oppose each other (opposing flow). It can be seen from Table1 that skin friction coefficient C_f and Sherwood number Sh decrease but Nusselt number Nu_x increases with the increases of the magnetic field parameter M on the other hand Nusselt number Nu_x and Sherwood number increase but skin friction coefficient C_f decreases with the increases of the suction parameter f_w. From Table2 we observe that if we increase Prandtl number Pr, skin friction coefficient, Nusselt number and Sherwood number increase but increasing of the Schmidt number Sc, skin friction coefficient C_f and Nusselt number Nu_x decrease but Sherwood number Sh increases. Table3 displays the effects of the heat source/sink parameter Q and the buoyancy parameter λ on the skin friction coefficient C_f, Nusselt number Nu_x and Sherwood number Sh. We observe that C_f, Nu_x and Sh increase with the increase of Q on the other hand skin friction coefficient and Sherwood number increase but Nusselt number decreases with the increase of the buoyancy parameter λ.

REFERENCES

1. Nachtsheim, P.R. and Swigert, P. (1965), Satisfiction of the asymptotic boundary conditions in numerical solution of the system of non-linear equations of boundary layer type, NASSA TND-3004.
2. D.T. Chin, Mass transfer to a continuous moving sheet electrode, J. Electrochem. Soc. 122(1975) 643.
3. R.S.R. Gorla, Unsteady mass transfer in the boundary layer on a continuous moving sheet electrode, J. Electrochem. Soc 125(1978) 865.
4. R.M. Griffith, Velocity temperature and concentration distributions during fibre spinning, Ind. Eng. Chem. Fundam. 3 (1964) 245.
5. L.E. Erickson, L.T. Fan, V.G. Fox, Heat and mass transfer on a moving continuous flat plate with suction or injection, Indust. Eng. Chem. Fundamentals 5 (1966) 19.
6. T. Altan, S. Oh, H. Gegel, Metal forming fundamentals and applications, American Society of Metals, Metals Park, OH, 1979.
7. E. G. Fisher, Extrusion of plastics, Wiley, New York, 1976.

8. Z. Tadmor, I. Klein, Engineering principles of plasticating extrusion processes, Polymer Science and Engineering Series, Van Nostrand Reinhold, New York, 1970.
9. Crane. L. J. Zeitschrift Angewandt Mathematik and Physik 1970, 21, 26
10. B.C. Sakiadis, Boundary layer behavior on continuous solid surfaces: I. Boundary-layer equations for two-dimensional and axisymmetric flow, AIChE J. 7(1)(1961) 7-28.
11. U.N. Das, R.K. Deka, V.M. Soundalgekar, Effects of mass transfer on flow past an impulsively started infinite vertical plate with constant heat flux and chemical reaction, Forsch. Ingenieurwes. 60(1994) 284.
12. H.I. Anderson, O.R. Hansen, B. Holmedal, Diffusion of a chemically reactive species from a stretching sheet, Int. J. Heat Mass Transfer 37 (1994) 659.
13. S.P. Anjalidevi, R. Kandasamy, Effects of chemical reaction heat and mass transfer on laminar flow along a semi infinite horizontal plate, Heat Mass Transfer 35 (1999) 465.
14. S.P. Anjalidevi, R. Kandasamy, Effects of chemical reaction heat and mass transfer on MHD flow past a semi infinite plate, Z.Angew. Math. Mech. 80 (2000) 697.
15. J.B. McLeod, K.R. Rajagopal, On the uniqueness of flow of a Navier-Stokes fluid due to a stretching boundary, Arch. Ration. Mech. Anal. 98 (1987) 386.
16. A.Raptis, C.Perdikis, Viscous flow over a non-linearly stretching sheet in the presence of a chemical reaction and magnetic field, Int. J. Non-linear Mechanics 41(2006) 527-529.
17. V.G. Fox, L.E. Erickson, L.T. Fan, Methods for solving the boundary layer equations for moving continuous flat surfaces with suction and injection, AIChE J. 14(1968) 726-736.
18. C.K. Chen, M.I. Char, Heat transfer of a continuous stretching surface with suction or blowing, J. Math. Ana. Appl. 135(1988) 568-580.
19. M.E. Ali, On thermal boundary layer on a power-law stretched surface with suction or injection, Internat. J. Heat Fluid Flow 16(4) (1995) 280-290.
20. E.Magyari, M.E. Ali, B.Keller, Heat and mass transfer characteristics of the self-similar boundary-layer flows induced by continuous surface stretched with rapidly decreasing velocities, Heat Mass Transfer 38 (2001) 65-74.
21. K. Vajravelu and A. Hadjinicolaou, Convective heat transfer in an electrically conducting fluid at a stretching surface with uniform free stream, Int. J. Engng. Sci. Vol. 35, No. 12/13, pp. 1237-1244, 1997
22. J. P. Holman, 2004, Heat Transfer, Ninth Edition, Tata McGraw-Hill Publishing Companies, Inc., pp. 316.